Journal of Chromatography B, 903 (2012) 118–125

Contents lists available at SciVerse ScienceDirect

Journal of Chromatography B

journal homepage: www.elsevier.com/locate/chromb

# Determination of phenylbutyric acid and its metabolite phenylacetic acid in different tissues of mouse by liquid chromatography with tandem mass spectrometry and its application in drug tissue distribution

Anu Marahatta[a], Bidur Bhandary[a], Mi-Rin Lee[a], Do-Sung Kim[a], Yong Chul Lee[b], So-Ri Kim[b], Hyung-Ryong Kim[c], Han-Jung Chae[a,*]

[a] Department of Pharmacology, School of Medicine, Chonbuk National University, Jeonju 560-182, South Korea
[b] Research Center for Pulmonary Disorders, Chonbuk National University Medical School, Jeonju, South Korea
[c] Department of Dental Pharmacology, School of Dentistry, Wonkwang University, Iksan, Chonbuk 570-749, South Korea

ARTICLE INFO

*Article history:*
Received 10 February 2012
Accepted 11 July 2012
Available online 20 July 2012

*Keywords:*
Phenylbutyric acid
Phenylacetic acid
Tissue distribution
Pharmacokinetic
Mass spectrometry

ABSTRACT

Endoplasmic reticulum (ER) stress is associated with various human diseases. Phenylbutyric acid (PBA) is a well-known chemical chaperone that regulates ER stress. The main objective of this study was to develop a simple, rapid, and sensitive method for the simultaneous determination of phenylbutyric acid and its metabolite, phenylacetic acid (PAA). A LC–MS/MS analysis using negative electrospray ionization was used. Samples were analyzed by multiple reaction monitoring (MRM) in 15 min of total run time, using d11-PBA and d7-PAA as internal standards. The limit of quantification was 1 μg/g for tissue and 0.8 μg/mL for plasma. Recoveries for plasma and tissues were higher than 81% for both PBA and PAA. The inter-day and intra-day accuracy and precision were within ±15%. We then further successfully validated this method by applying it to determine the tissue distribution of PBA and its metabolite PAA after i.p. injection of PBA at a dose of 500 mg/kg in mice. The maximum concentrations of PBA and PAA in plasma and tissues were seen at 15 min and 45 min, respectively. The PBA plasma concentration was 15-fold higher than the concentration in the kidney, whereas the PAA plasma concentration was 6-fold higher than the concentration in the liver. The area under the curve decreased in the order of plasma > kidney > liver > heart > muscle > lung for PBA and plasma > liver > kidney > heart > muscle > lung for PAA. The tissue to plasma ratio ranged from 0.007 to 0.063 for PBA and 0.016 to 0.109 for PAA. In summary, the LC–ESI-MS method developed in this study is simple, sensitive and reliable.



## 1. Introduction

Endoplasmic reticulum (ER) stresses are caused by accumulation of unfolded/misfolded proteins and other conditions affecting ER homeostasis. Physiological or pathological conditions such as protein folding, transport, degradation, calcium homeostasis are altered during ER stress [1]. Disturbances in ER homeostasis produce prolonged activation of unfolded protein response that may contribute to the pathogenesis of many diseases [2]. ER stress has been found to be associated with neurodegenerative, ischemic heart, diabetic kidney, autoimmune myositis, lung and fatty liver disease [3–7]. Sodium phenylbutyrate (PBA) is a chemical chaperone and a histone deacetylase inhibitor that suppresses the ER stress response [8]. A number of studies have shown that PBA (Fig. 1a) plays a protective role in multiple sclerosis [9], cerebral ischemic injury [10], spinal cord ischemia [11], and restores glucose homeostasis in a mouse model of type-2 diabetes [7], cystic fibrosis, and thalassemia [12,13]. Thus, assessing the amount of PBA in various tissues is an important issue.

PBA is a pro-drug which is converted into phenylacetic acid (PAA) (Fig. 1b) by β-oxidation in mitochondria of the liver and kidney, which become conjugated with glutamine to form phenylacetylglutamine (PAGN) or phenybutyrylglutamine (PBGN) [14]. The metabolite of PBA is finally excreted via the urine [15,16]. The majority of the administered compound (approximately 80–100%) is excreted as phenylacetylglutamine within 24 h. The cumulative excretion of PBA + PAA + PAG + PBGN accounts for only about half of the amount of PBA ingested [17]. PBA and PAA also can penetrate the cerebrospinal fluid [18].

*Abbreviations:* AUC, area under curve; d11-PBA, d11-phenylbutyric acid; d7-PAA, d7-phenylacetic acid; PAA, phenylacetic acid; PBA, phenylbutyric acid; RSD, relative standard deviation; PAGN, phenylacetylglutamine; PBGN, phenybutyrylglutamine; QC, quality control; i.p., intraperitoneal.

* Corresponding author. Tel.: +82 63 270 3092; fax: +82 63 275 2855.
*E-mail addresses:* hjchae@chonbuk.ac.kr, hjchae@jbnu.ac.kr (H.-J. Chae).

1570-0232/$ – see front matter © 2012 Elsevier B.V. All rights reserved.
http://dx.doi.org/10.1016/j.jchromb.2012.07.004

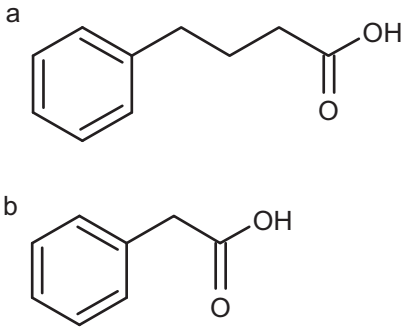


**Fig. 1.** (a) Chemical structure of PBA. (b) Chemical structure of PAA.

Several analytical methods including high performance liquid chromatography (HPLC) with UV [19], diode array detector (DAD) [20], and gas chromatography [21] have been used for the analysis of PBA and PAA in human and rat plasma. The HPLC assay for the analysis of PAA and PBA in the plasma has limited sensitivity. However, simultaneous determination of PBA and PAA in tissue samples has not been attempted up to date, and only a few methods are available to analyze plasma samples using LC–MS/MS.

The main objectives of the study were (1) to develop and validate a simple, rapid, sensitive method for the simultaneous determination of PBA and its metabolite PAA in mouse plasma and (2) to determine the tissue distribution characteristics of PBA. Pharmacokinetics and tissue distribution of PBA and PAA can provide useful information for clinical practice.

## 2. Experimental

### 2.1. Chemicals and reagents

PBA (98% purity) was purchased from Santa Cruz Biotechnology, Inc. (Santa Cruz, CA, USA). PAA (99% purity) was obtained from Sigma (St. Louis, MO, USA). d11-Phenylbutyric acid (d11-PBA), 99.4 atom % D, and d7-phenylacetic acid (d7-PAA), 98 atom % D, were obtained from CDN Isotopes (Pointe-Claire Quebec, Canada). Water was purified by a Milli-Q system from Millipore (Bedford, MA, USA). LC–MS grade acetonitrile, methanol and formic acid were from Fischer Scientific (Fai Lawn, NJ, USA). Ethanol was obtained from Merck (Darmstadt, Germany).

### 2.2. Preparation of calibration standards and quality control (QC) samples

Stock solutions of PBA and PAA (1 mg/mL) were prepared by dissolving 10 mg of the drug in 10 mL of 70% ethanol and stored at −4 °C. Deuterated labeled analytes were dissolved in methanol and used as internal standards (IS). Calibration standards were prepared by spiking working standard solutions and IS into 100 μL of blank mouse plasma or different tissue homogenates of untreated mouse. The final concentrations of the standard curve samples were 1–50 μg/mL for the plasma and 1–50 μg/g for the tissue. The IS concentration is 2.5 μg/mL in each sample. QC samples were prepared at three concentrations (1, 10, and 50 μg/mL for plasma or 1, 10, and 50 μg/g for tissue). The standard calibration samples and QC samples were stored at −20 °C until analysis.

### 2.3. Animals

C57B/L mice were obtained from Damul Science (Deajeon, South Korea). The animals were kept in a fully acclimatized room at constant temperature and humidity on a 24 light/dark cycle. The animals had free access to food and water. Mice were given a single dose of PBA (500 mg/kg, dissolved in phosphate buffered saline) intraperitoneally (i.p.). Blood and tissue samples were collected at 0, 0.25, 0.5, 0.75, 1, 1.5, 2, 3, and 4 h and stored at −80 °C. Six animals were sacrificed at each time point. The study was approved by the animal use committee at Chonbuk National University, South Korea.

**Table 1**
Multiple reaction monitoring (MRM) transition and conditions for all compounds and their deuterated analogs.

| Compound | Precursor ion (m/z) | Product ion (m/z) | Collision energy (eV) |
|---|---|---|---|
| Phenylbutyric acid | 163.1 | 91.5 | 12 |
| Phenylacetic acid | 135.3 | 91.3 | 12 |
| d11-Phenylbutyric acid | 174.2 | 98.2 | 12 |
| d7-Phenylacetic acid | 142.2 | 98.0 | 12 |

### 2.4. Chromatographic conditions

HPLC separation was performed on an Agilent 1100 system (Agilent, Palo Alto, CA, USA). Chromatography separation was performed using a Kinetex C18 column (50 × 2.10 mm internal diameter and 2.6 μm particle size). PBA, PAA, and IS were separated by a gradient elution. The mobile phase was composed of solvent A, water and solvent B, acetonitrile, and both solvents contained 0.1% formic acid. The gradient run started with 25% solvent B for 1 min and then raised to 100% for 6 min, where it remained for another 1 min, and then returned to 25% in 10 min, then maintained for 5 min. Chromatography was performed at 30 °C with a flow rate of 0.23 mL/min, and the run time was 15 min. The injection volume was 2 μL for each sample.

### 2.5. Mass spectrometer conditions

An Agilent Technologies 6410 triple quadruple mass spectrometer equipped with electrospray ionization (ESI) in the negative ionization mode was used. The following conditions were found to be optimal for analysis: capillary voltage 4 kV, gas temperature 300 °C, and gas flow 10 L/min. Samples were analyzed by multiple reaction monitoring (MRM). The precursor ions, product ions, and MS/MS parameters are reported in Table 1. Mass hunter software was used to control the LC–MS/MS system and data analysis. Working solutions of PBA and PAA were obtained by diluting the stock solutions with methanol.

### 2.6. Sample preparation procedure

#### 2.6.1. Plasma

To a 100 μL plasma sample, 50 μL of IS and 850 μL of acetonitrile were added to precipitate the proteins in the sample. The resulting solution was vortexed for 30 s and centrifuged at 13,000 × *g* for 20 min. The supernatant was transferred to a HPLC vial and injected.

#### 2.6.2. Tissue samples (Liver, heart, kidney, muscle, and lung)

Tissues were chopped into small pieces using scissors and were homogenized in a saline solution (600 mg/mL) using a Polytron PT 1200 C homogenizer (Kinematica Inc., Switzerland). To 100 μL of the above tissue homogenates, 50 μL of IS and 850 μL of acetonitrile were added. The resulting solution was mixed by vortexing for 30 s. The solution was then centrifuged at 13,000 × *g* for 20 min at 4 °C, and an aliquot of the supernatant was used for analysis.

### 2.7. Pharmacokinetic methods

Plasma concentration–time curves were evaluated by non-compartmental analysis using WinNonlin®, version 5.2 (Pharsight

Corp, Mountain View, CA, USA). The maximal drug concentration ($C_{max}$, μg/mL or μg/g) and the time of maximal peak concentration ($t_{max}$, h) were derived directly from the experimental data. The area under the concentration–time curves (AUC, h μg/mL or h μg/g) were calculated by the linear trapezoid rule. The estimation of $AUC_{0-t}$ ($t$ = 4 h for PAA) was obtained by using the linear trapezoidal rule. Half-life ($t_{1/2}$) values were calculated using the equations: $t_{1/2} = 0.693/\lambda$. The mean residence time (MRT, h) was calculated as AUMC/AUC (AUMC: area under the first moment curve).

### 2.8. Matrix effect and recovery

Matrix effect was evaluated by comparing the mean peak areas of PBA and PAA from the spike, after protein precipitation (B) with those of the standard solution in mobile phase (A). The ratio (B/A × 100)% was calculated to evaluate the matrix effect. The matrix effect for the IS was also evaluated at the concentration used in the analysis (2.5 μg/mL). Extraction recovery tests were performed by comparing the peak areas of the sample prepared by plasma and tissue extraction and those of directly injected standards. Recoveries at three concentrations for plasma and tissue samples were evaluated.

### 2.9. Limit of detection (LOD) and limit of quantification (LOQ)

LOD and LOQ were estimated from signal to noise ratios. LOD was defined as the lowest concentration level giving a peak area of three times the noise. LOQ was defined as the lowest concentration that provided a peak area with signal to noise ratio >10.

### 2.10. Linearity

Calibration curves of PBA and PAA in plasma and tissue samples were established over a concentration range of 1–50 μg/mL for plasma and 1–50 μg/g for tissue.

### 2.11. Precision and accuracy

Intra-day and inter-day accuracy (relative error) and precision (% relative standard deviation or RSD) were assessed by analyzing sample concentrations at 5, 10, and 25 μg/mL for each drug. To determine the intra-day precision of the method, three different concentrations of plasma and each tissue were analyzed five times on the same day. The inter-day precision and accuracy were evaluated five times in another independent sample extracted on three separate days. Accuracy was calculated as the percent deviation from the nominal concentration.

## 3. Results and discussions

### 3.1. Mass Spectrometry

Various concentrations of acetonitrile and water were evaluated using the LC–ESI–MS/MS system at a flow rate 0.23 mL/min. The above method is sensitive, rapid, robust, and has the ability to separate PBA, PAA, and the internal standard without interference from endogenous compounds. To control the matrix effects, this study used stable isotope labeled analogs, which are believed to be the most appropriate IS for quantitative LC–MS/MS analysis. IS does not show any suppressing effect on the analyte ions in the LC–MS/MS analysis. To determine the analytes using the selected MRM mode, full scan and product ion spectra of PBA, PAA, and IS were investigated. ESI analysis showed that PBA, PAA, d11-PBA, and d7-PAA formed the deprotonated molecules $[M-H]^-$ of m/z 163.1, 135.3, 174.2, and 142.2 in full scan spectra. The most abundant ion in the product ion mass spectrum was at 91.5 for PBA, followed by 91.3 for PAA, 98.2 for d11-PBA, and 98 for d7-PAA. The capillary temperature and the spray voltage did not significantly influence the MS behavior of the analytes and were maintained at the auto-tuned values. Different collision energies were assessed, and the results showed that 12 V collision energy increases the fragmentation processes. The MRM transitions of m/z 163.1 → 91.5 for PBA, 135.3 → 91.3 for PAA, 174.2 → 98.2 for d11-PBA, and 142.2 → 98 for d7-PAA were used to obtain the maximum sensitivity.

### 3.2. Liquid chromatography – mobile phase selection

The HPLC mobile phase was examined using various compositions of acetonitrile–water by varying the percentages to provide the best sensitivity and peak shape for the analysis. Different percentages of formic acid (0.1–0.9%) were also tested to find the best sensitivity. The addition of 0.1% formic acid in the mobile phase enhanced the sensitivity. Acetonitrile–water containing 0.1% formic acid in the mobile phase was found to be optimal for the present study. Under the above analytical conditions, the retention times were 1.87, 1.94, 4.8, and 5.4 min for d7-PAA, PAA, d11-PBA, and d11-PBA, respectively, and the total run time was 15 min (Fig. 2). Several HPLC methods have been applied to analyze PBA, PAA in plasma [20,21]. The analytical run times of all the above studies were 45 min, which is very long compared to our method. Thus, the LC–MS/MS method developed in this study shows advantages in both analytical analysis time and sensitivity.

### 3.3. Extraction procedure

Liquid–liquid, solid phase extraction (SPE) and protein precipitation (PPT) are the most commonly used sample preparation techniques. In this study, PPT was used for sample preparation because it is a simple, easy, and rapid sample clean-up procedure. Extraction of PBA and PAA from various tissues was achieved using different organic solvents such as methanol, methanol/water, acetonitrile, and acetonitrile/water. The test results showed that acetonitrile yielded higher analytes recovery than other solvents. The recovery yields using methanol (less than 70%), methanol/water or acetonitrile/water (less than 55%) were found to be lower than for acetonitrile (greater than 81%). In a previously published method, methanol was used as the extraction solvent [18]. Higher extraction efficiency was obtained using acetonitrile, so it was selected as the extraction solvent.

### 3.4. Method validation

#### 3.4.1. Linearity

Standard curves over a broad concentration range (1–50 μg/mL for plasma or 1–50 μg/g for tissue) were prepared in the plasma and various tissues. A good linear relationship between the peak area and the drug concentration was observed for all tissues and plasma. The standard curves of the peak area ($y$) to the concentration ($c$) were constructed using the $1/x^2$ weighted linear least squares regression model. The standard curves, correlation coefficients, and linear ranges of PBA and PAA in plasma and tissue samples are listed in Table 2. The limit of quantification was 1 μg/g for all tissues and 0.8 μg/mL for plasma. MA Carducci et al. reported LOQ was 5 μg/mL for plasma [20].

#### 3.4.2. Specificity

This method developed in this study had high specificity because only a fragment ion derived from the $[M-H]^-$ ion of the analytes of interest was monitored. Blank plasma samples ($n$ = 6) were analyzed to assess the specificity. Fig. 2 represents a chromatogram of a blank sample. No interference peaks were found in MRM profiles

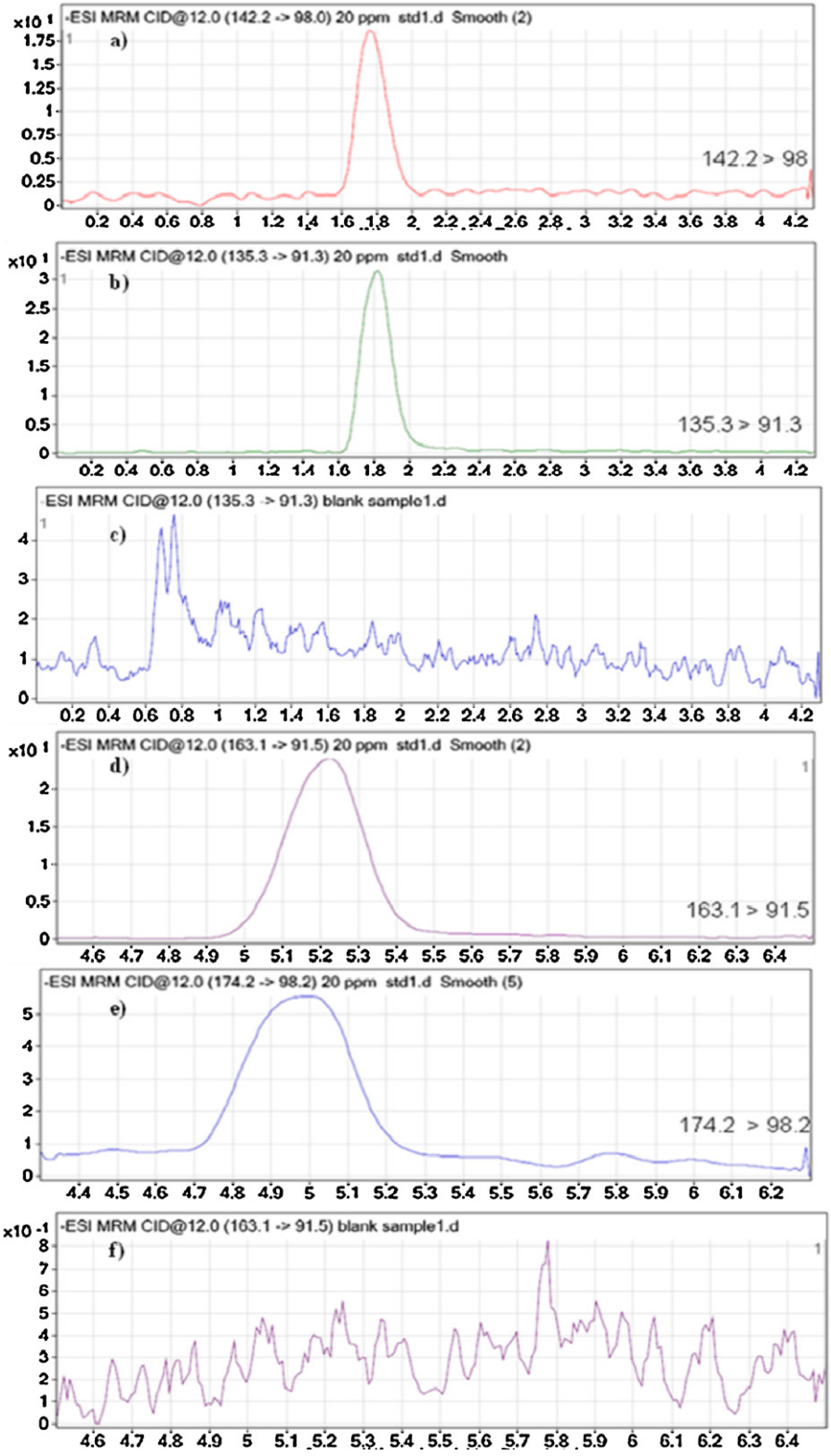


**Fig. 2.** Multiple Reaction Monitoring chromatograms of (a) d7-PAA, (b) PAA, (c) blank plasma (PAA), (d) PBA, (e) d11-PBA and (f) blank plasma (PBA).

of the blank plasma or tissue observed at the retention time of the analytes.

*3.4.3. Matrix effect and recovery*

In the matrix effect evaluation, the observed variation did not exceed the range 85–115%. Thus, ion suppression or enhancement was not significant with the HPLC–MS/MS method. The matrix effect ratio obtained for IS were 95.445 ± 1.543% for d11-PBA and 96.893 ± 3.624% for d7-PAA at 2.5 μg/mL. The recoveries of PBA and PAA from plasma and various tissues were measured at three concentrations by comparing the peak areas from the extracted tissues with those obtained by direct injection of the standard solutions at the same concentrations. Table 3 shows the % recoveries and matrix effect of PBA and PAA obtained from plasma and various tissue

**Table 2**
Standard curves, correlation coefficients, and linear range of PBA and PAA in plasma and tissue samples ($n = 5$).

| Sample | Equation | | $r^2$ | | Linear range (μg/mL or μg/g) |
|---|---|---|---|---|---|
| | PBA | PAA | PBA | PAA | |
| Plasma | $y = 0.221x - 0.104$ | $y = 0.116x + 0.228$ | 0.991 | 0.993 | 1–50 |
| Liver | $y = 0.202x + 0.274$ | $y = 0.107x + 0.152$ | 0.994 | 0.992 | 1–50 |
| Heart | $y = 0.194x - 0.220$ | $y = 0.099x + 0.206$ | 0.994 | 0.996 | 1–50 |
| Kidney | $y = 0.204x + 0.348$ | $y = 0.106x + 0.174$ | 0.992 | 0.990 | 1–50 |
| Muscle | $y = 0.210x + 0.283$ | $y = 0.119x + 0.175$ | 0.994 | 0.992 | 1–50 |
| Lung | $y = 0.190x + 0.114$ | $y = 0.102x + 0.031$ | 0.997 | 0.995 | 1–50 |

samples. Recoveries were 82.529 ± 7.110% to 105.766 ± 0.255% for PBA and 81.313 ± 1.610% to 102.769 ± 2.519% for PAA. Recoveries were higher than the previously reported method [21].

### 3.4.4. Precision and accuracy

Precision and accuracy were validated at three concentrations as shown in Table 4. The intra-day precision for plasma was 0.845–6.754% for PBA and 3.032–6.833% for PAA. The intra-day accuracy ranged from −10.684 to −5.400% for PBA and −3.990 to −1.396% for PAA. Similarly, the inter-day accuracy ranged from −9.676 to −5.100% for PBA and −1.860 to −1.240% for PAA. The inter-day precision was 0.599–4.235% and 1.605–2.070%, for PBA and PAA respectively.

For tissue homogenate, the intra-day precision was in the ranged 0.333–4.919% for PBA and 0.236–8.105% for PAA. Inter-day precision was 0.042–6.579% for PBA and 1.605–8.745% for PAA. Intra-day accuracy ranged from −9.900 to −1.724% and −10.408 to −2.200%, whereas inter-day accuracy varied from −10.712 to −3.160% and −10.484 to 1.612%, for PBA and PAA respectively. The intra-day and inter-day variation, as well as the accuracy, were within the acceptable range, confirming that the current method was reproducible and accurate.

### 3.5. Application of the method

The method was applied to the analysis of plasma and tissue samples obtained from the pharmacokinetic study. C57B/L mice were given a single dose of PBA (500 mg/kg) i.p. Although the oral and i.p. dose of 500 mg/kg PBA to mice is generally high, but the concentration of the drug is routinely used in animal studies [22,23]. Even a higher dose was used in the treatment of Huntington's disease in mice [23]. Blood and tissue samples were collected at 0, 0.25, 0.5, 0.75, 1, 1.5, 2, 3, and 4 h. The concentration–time profiles of PBA and PAA in plasma are shown in Fig. 3. PBA and PAA concentrations were higher in plasma than in the tissue.

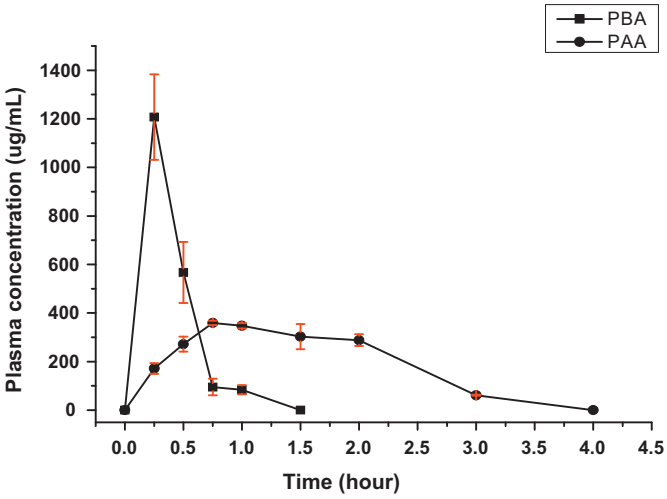


**Fig. 3.** Pharmacokinetic profiles of PBA and PAA in mouse plasma following i.p. administration of a single dose (500 mg/kg) of PBA ($n = 6$).

Pharmacokinetic analyses of PBA and PAA in mouse plasma and tissues including lung, liver, heart, kidney and muscle are summarized in Tables 5 and 6, respectively. The highest PBA tissue concentration was observed in the kidney, followed by liver, heart, muscle, and lung. The tissue concentration of PAA was highest in the liver followed by kidney, muscle, heart, and lung. Maximum concentrations of PBA for plasma and tissues examined were seen at 15 min after administration, whereas the highest concentration of PAA was found at 45 min. Kasumov et al., have reported

**Table 3**
Recovery of PBA and PAA in plasma and different tissues ($n = 6$).

| Sample | Concentration (μg/mL or μg/g) | Recovery (%) | | Matrix effect (%) | |
|---|---|---|---|---|---|
| | | PBA ± SD | PAA ± SD | PBA ± SD | PAA ± SD |
| Plasma | 1 | 105.766 ± 0.255 | 99.638 ± 3.624 | 101.288 ± 0.746 | 97.343 ± 0.511 |
| | 10 | 101.741 ± 6.135 | 102.769 ± 2.519 | 100.516 ± 0.023 | 99.746 ± 0.006 |
| | 50 | 101.777 ± 7.071 | 101.879 ± 7.879 | 96.816 ± 0.045 | 97.922 ± 2.037 |
| Liver | 5 | 86.595 ± 5.933 | 81.866 ± 3.572 | 101.331 ± 2.547 | 98.559 ± 0.041 |
| | 10 | 89.264 ± 0.432 | 88.589 ± 4.419 | 95.592 ± 0.186 | 92.575 ± 0.011 |
| | 25 | 82.529 ± 7.110 | 97.855 ± 3.985 | 95.364 ± 0.048 | 99.938 ± 2.706 |
| Heart | 5 | 101.057 ± 7.342 | 98.500 ± 0.200 | 100.553 ± 3.891 | 95.719 ± 1.330 |
| | 10 | 98.404 ± 0.594 | 98.458 ± 2.177 | 96.002 ± 0.037 | 97.775 ± 0.246 |
| | 25 | 98.324 ± 0.647 | 99.008 ± 4.733 | 96.782 ± 0.018 | 93.861 ± 3.070 |
| Kidney | 5 | 100.938 ± 2.220 | 85.183 ± 5.065 | 94.564 ± 4.247 | 105.185 ± 0.829 |
| | 10 | 94.124 ± 0.855 | 93.038 ± 2.194 | 99.889 ± 0.287 | 96.001 ± 0.376 |
| | 25 | 94.171 ± 2.026 | 92.382 ± 0.500 | 94.478 ± 0.018 | 103.275 ± 2.915 |
| Muscle | 5 | 101.712 ± 3.246 | 100.285 ± 5.207 | 98.252 ± 2.832 | 99.978 ± 3.514 |
| | 10 | 97.599 ± 1.014 | 92.299 ± 8.110 | 92.631 ± 0.325 | 94.172 ± 0.031 |
| | 25 | 88.850 ± 3.310 | 81.313 ± 1.610 | 96.268 ± 0.016 | 96.696 ± 1.196 |
| Lung | 5 | 98.528 ± 2.426 | 86.829 ± 2.989 | 99.644 ± 2.074 | 99.625 ± 1.255 |
| | 10 | 90.986 ± 5.640 | 97.128 ± 2.825 | 98.177 ± 0.517 | 96.388 ± 0.073 |
| | 25 | 88.661 ± 3.409 | 89.882 ± 6.297 | 93.383 ± 2.406 | 90.935 ± 1.028 |

**Table 4**
Intra day and inter day precision and accuracy.

| Sample | Concentration (μg/mL or g) | Intra day ($n = 3$) | | | | | | Inter day ($n = 3$) | | | | | |
|---|---|---|---|---|---|---|---|---|---|---|---|---|---|
| | | PBA ± SD | Precision (%RSD) | Accuracy (%bias) | PAA ± SD | Precision (%RSD) | Accuracy (%bias) | PBA ± SD | Precision (%RSD) | Accuracy (%bias) | PAA ± SD | Precision (%RSD) | Accuracy (%bias) |
| Plasma | 1 | 0.946 ± 0.041 | 4.412 | −5.400 | 0.951 ± 0.028 | 3.032 | −4.900 | 0.949 ± 0.569 | 0.599 | −5.100 | 0.994 ± 1.726 | 1.735 | −0.600 |
| | 10 | 9.014 ± 0.076 | 0.845 | −9.860 | 9.601 ± 0.656 | 6.833 | −3.990 | 9.448 ± 4.002 | 4.235 | −5.520 | 10.124 ± 2.102 | 2.070 | 1.240 |
| | 25 | 22.329 ± 1.508 | 6.754 | −10.684 | 24.651 ± 4.849 | 4.849 | −1.396 | 22.581 ± 3.131 | 3.467 | −9.676 | 24.540 ± 1.476 | 1.605 | −1.860 |
| Liver | 1 | 0.957 ± 0.032 | 3.421 | −4.300 | 0.911 ± 0.005 | 0.573 | −8.900 | 0.966 ± 5.486 | 5.676 | −3.360 | 0.912 ± 4.699 | 5.151 | −8.800 |
| | 10 | 9.060 ± 0.445 | 4.919 | −9.400 | 9.720 ± 0.182 | 1.869 | −2.800 | 9.431 ± 2.573 | 2.727 | −5.690 | 9.388 ± 2.633 | 2.805 | −6.120 |
| | 25 | 23.329 ± 0.939 | 4.026 | −6.684 | 24.227 ± 0.875 | 3.61 | −3.092 | 22.429 ± 0.507 | 2.264 | −10.284 | 25.403 ± 1.388 | 5.466 | 1.612 |
| Heart | 1 | 0.922 ± 0.019 | 2.050 | −7.800 | 0.947 ± 0.077 | 8.105 | −5.300 | 0.913 ± 2.709 | 2.966 | −8.700 | 0.952 ± 3.204 | 3.364 | −4.800 |
| | 10 | 9.281 ± 0.085 | 0.922 | −7.190 | 9.395 ± 0.079 | 0.841 | −6.050 | 9.011 ± 3.869 | 4.294 | −9.890 | 9.622 ± 5.466 | 5.681 | −3.780 |
| | 25 | 23.731 ± 0.866 | 3.652 | −5.076 | 23.086 ± 0.482 | 0.236 | −7.656 | 23.037 ± 0.255 | 2.188 | −6.116 | 22.379 ± 1.957 | 8.745 | −10.484 |
| Kidney | 1 | 0.901 ± 0.026 | 2.968 | −9.900 | 0.978 ± 0.075 | 7.669 | −2.200 | 0.944 ± 3.971 | 0.042 | −5.600 | 0.991 ± 8.627 | 8.705 | −0.900 |
| | 10 | 9.081 ± 0.429 | 4.863 | −9.190 | 9.560 ± 0.631 | 6.601 | −4.400 | 9.641 ± 6.343 | 6.579 | −3.581 | 9.976 ± 2.043 | 2.047 | −0.240 |
| | 25 | 24.569 ± 0.627 | 2.552 | −1.724 | 23.363 ± 1.423 | 6.092 | −6.548 | 23.471 ± 0.255 | 1.087 | −6.116 | 23.072 ± 1.317 | 5.708 | −7.712 |
| Muscle | 1 | 0.922 ± 0.003 | 0.333 | −7.800 | 0.978 ± 0.012 | 1.274 | −2.200 | 0.954 ± 4.825 | 5.056 | −4.570 | 1.010 ± 6.429 | 6.941 | 1.000 |
| | 10 | 9.536 ± 0.195 | 2.045 | −4.640 | 9.448 ± 0.348 | 3.678 | −5.580 | 9.253 ± 2.307 | 2.493 | −7.470 | 9.100 ± 4.538 | 4.986 | −9.000 |
| | 25 | 22.888 ± 0.675 | 2.949 | −8.448 | 23.281 ± 0.483 | 2.072 | −6.876 | 22.322 ± 0.416 | 1.866 | −10.712 | 23.463 ± 1.247 | 2.076 | −6.150 |
| Lung | 1 | 0.936 ± 0.019 | 2.049 | −6.360 | 0.908 ± 0.067 | 7.423 | −9.200 | 0.942 ± 4.546 | 4.827 | −5.839 | 0.926 ± 6.429 | 6.941 | −7.400 |
| | 10 | 9.078 ± 0.429 | 4.732 | −9.220 | 9.143 ± 0.106 | 1.160 | −8.570 | 9.684 ± 4.326 | 4.467 | −3.160 | 9.190 ± 1.476 | 1.605 | −8.100 |
| | 25 | 22.858 ± 0.634 | 2.949 | −8.568 | 22.398 ± 0.337 | 1.504 | −10.408 | 22.716 ± 0.468 | 2.062 | −9.136 | 22.880 ± 0.837 | 3.658 | −8.480 |

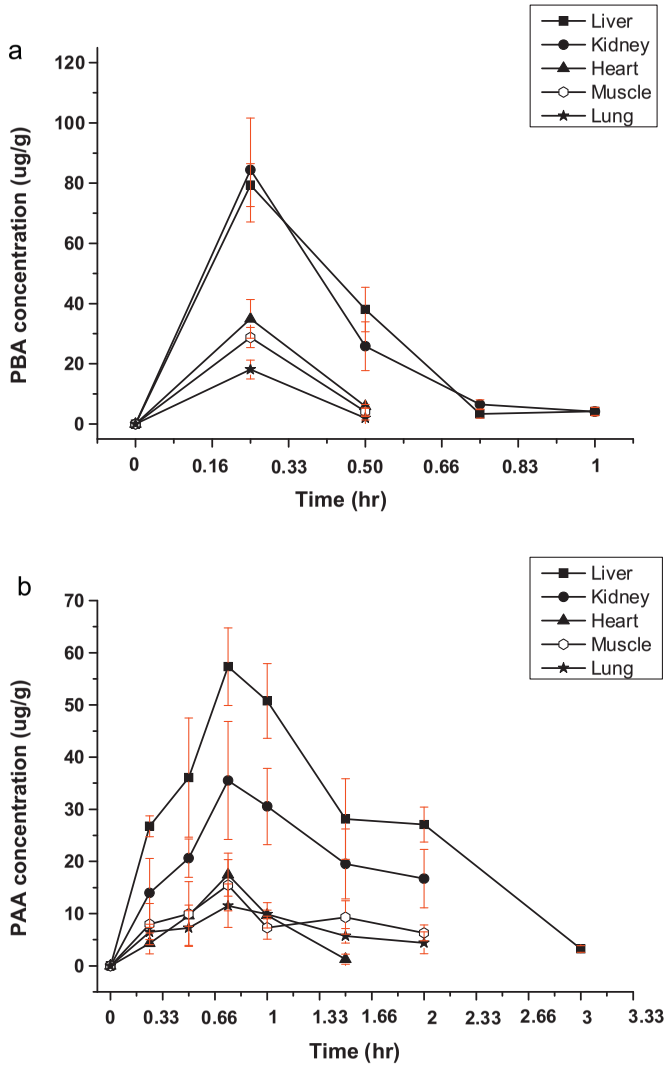


**Fig. 4.** (a) Concentrations (mean ± S.D.) versus time profiles of PBA in the liver, kidney, heart, lung and muscle after a single i.p. injection of 500 mg/kg of PBA to mouse ($n = 6$). (b) Concentrations (mean ± S.D.) versus time profiles of PAA in the liver, kidney, heart, lung and muscle after a single i.p. injection of 500 mg/kg of PBA to mouse ($n = 6$).

that $t_{max}$ for PBA is seen at 30 min in plasma by using gavaged method [17]. Pharmacokinetic study with patients having recurrent malignant gliomas by Surasak et al., showed $t_{max}$ at 1.5 h, $C_{max}$ 1225 μM for PBA, and $t_{max}$ at 3.3 h, $C_{max}$ 617 μM for PAA in plasma [19]. In their study, the human subjects were orally administered with PBA 27 g/day divided in three doses administered at administration times. Experimental conditions as subject, dose, and route of administration in the study by Surasak et al., and Kasumov et al., were different than our experimental conditions. Hence, the pharmacokinetic parameters were also different. The half life of PBA was less than 30 min in plasma and tissues. The half life of PAA after i.p. injection of PBA ranged from 0.080 to 0.455 h. In the case of PAA, the longest half life was observed in plasma, followed by the lung, kidney, muscle, heart, and liver. Clearance was about 0.030–27.875 mL/h for PBA and 0.130–13.765 mL/h for PAA. The mean plasma metabolite to parent drug AUC ratio was 1.343 ± 0.676, consistent with previous reports [17,19]. The mean metabolite to parent drug AUC ratio for the tissue was 2.045 ± 0.877 for liver, 3.118 ± 1.665 for lung, 0.811 ± 0.473 for kidney, 2.119 ± 0.847 for muscle, and 1.992 ± 1.377 for heart.

**Table 5**
Pharmacokinetics of PBA in mouse following i.p. administration at a dose 500 mg/kg ($n = 6$).

| Sample | $C_{max}$ (μg/mL or g) | $T_{max}$ (h) | AUC (h μg/mL or g) | $t_{1/2}$ (h) | $CL_{(obs)}$ (mL/h) | MRT (h) | $AUC_{PAA}$:$AUC_{PBA}$ | $AUC_{tissue}$: $AUC_{plasma}$ |
|---|---|---|---|---|---|---|---|---|
| Plasma | 1207.411 ± 175.883 | 0.250 ± 0.000 | 474.971 ± 166.343 | 0.455 ± 0.491 | 0.304 ± 0.124 | 0.357 ± 0.036 | 1.343 ± 0.676 | |
| Liver | 79.345 ± 17.501 | 0.250 ± 0.000 | 29.064 ± 8.805 | 0.363 ± 0.416 | 0.003 ± 0.001 | 0.336 ± 0.026 | 2.045 ± 0.877 | 0.061 |
| Lung | 18.107 ± 7.625 | 0.250 ± 0.000 | 3.618 ± 2.244 | 0.080 ± 0.027 | 27.875 ± 9.789 | 0.256 ± 0.009 | 3.118 ± 1.665 | 0.007 |
| Kidney | 84.370 ± 42.254 | 0.250 ± 0.000 | 30.246 ± 13.094 | 0.167 ± 0.095 | 3.906 ± 0.568 | 0.350 ± 0.046 | 0.811 ± 0.473 | 0.063 |
| Muscle | 27.870 ± 7.019 | 0.250 ± 0.000 | 6.541 ± 2.405 | 0.081 ± 0.030 | 19.330 ± 6.165 | 0.261 ± 0.010 | 2.119 ± 0.847 | 0.013 |
| Heart | 34.923 ± 15.739 | 0.250 ± 0.000 | 7.191 ± 5.105 | 0.122 ± 0.077 | 13.824 ± 7.056 | 0.261 ± 0.017 | 1.992 ± 1.377 | 0.015 |

**Table 6**
Pharmacokinetics of PAA in mouse ($n = 6$).

| Sample | $C_{max}$ (μg/mL or g) | $T_{max}$ (h) | AUC (h μg/mL or g) | $t_{1/2}$ (h) | $CL_{(obs)}$ (mL/h) | MRT (h) | $AUC_{tissue}$: $AUC_{plasma}$ |
|---|---|---|---|---|---|---|---|
| Plasma | 359.492 ± 21.927 | 0.750 ± 0.000 | 556.851 ± 110.695 | 2.438 ± 1.506 | 0.130 ± 0.084 | 1.093 ± 0.177 | |
| Liver | 58.000 ± 9.861 | 0.812 ± 0.045 | 60.795 ± 26.174 | 0.233 ± 0.045 | 0.161 ± 9.717 | 0.955 ± 0.360 | 0.109 |
| Lung | 13.513 ± 6.001 | 0.875 ± 0.375 | 11.486 ± 4.262 | 1.561 ± 1.366 | 7.173 ± 2.967 | 0.875 ± 0.266 | 0.020 |
| Kidney | 34.962 ± 23.106 | 0.800 ± 0.485 | 34.763 ± 21.635 | 0.698 ± 0.580 | 2.673 ± 0.966 | 0.947 ± 0.204 | 0.062 |
| Muscle | 15.871 ± 6.628 | 0.900 ± 0.418 | 13.830 ± 5.120 | 0.321 ± 0.209 | 8.164 ± 2.503 | 1.018 ± 0.202 | 0.024 |
| Heart | 17.423 ± 8.287 | 0.750 ± 0.000 | 9.071 ± 3.234 | 0.319 ± 0.230 | 13.765 ± 9.027 | 0.684 ± 0.016 | 0.016 |

To the best of our knowledge, our study is the first to report on the tissue distribution of PBA and its metabolite (PAA) in mice. PBA and PAA tissue distribution were shown in Fig. 4. For PBA, the plasma concentration was 15-fold higher than the tissue concentration of the kidney, whereas PAA plasma concentration was 6-fold higher than the concentration in the liver. The AUC decreased in the order of plasma > kidney > liver > heart > muscle > lung for PBA; and plasma > liver > kidney > heart > muscle > lung for PAA (Fig. 5). The PAA concentration was higher in the liver and kidney because PBA is converted to PAA by mitochondria of the liver and kidney. The mean ratio of PBA in the tissue to plasma (expressed as AUC) was 0.061 for liver, 0.007 for lung, 0.063 for kidney, 0.013 for muscle, and 0.015 for heart. The mean ratio of PAA in the tissue to plasma was 0.109 for liver, 0.020 for lung, 0.062 for kidney, 0.024 for muscle, and 0.016 for heart. PAA metabolites were not detected in plasma or tissues after 4 h.

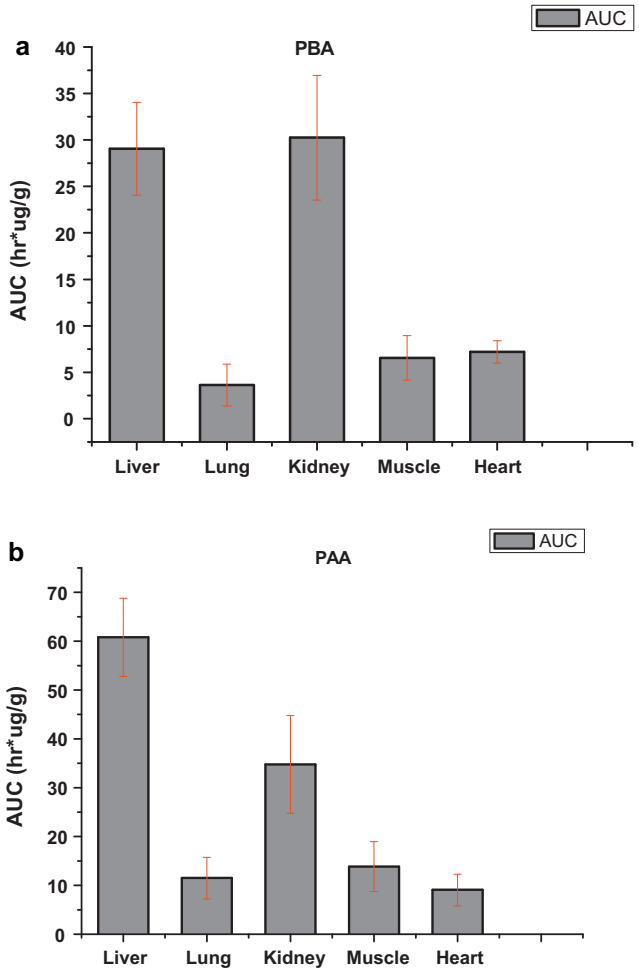


**Fig. 5.** (a) Area under the curve of PBA in different tissues after i.p. injection of PBA to mouse ($n = 6$). (b) Area under the curve of PAA in different tissues after i.p. injection of PBA to mouse ($n = 6$).

In this study, we evaluated pharmacokinetic profiles of a chemical chaperone, PBA and its metabolite, PAA, which is known as an antitumor agent. According to previous studies, PAA is further metabolized to PAGN and PBGN and finally excreted through the urine/bile [14–16]. A study by Kasumov et al. has presented the cumulative excretions of PBA, PAA, PAGN and PBGN accounts for 50% of total injected [17]. Hence, further investigation of PBA metabolites other than PAA and their excretion parameters are needed to be studied in future.

## 4. Conclusion

A simple, sensitive, reliable, and rapid LC/MS/MS method has been developed and validated for simultaneous analysis of PBA and PAA. This method has been applied to study the tissue distribution of PBA and PAA in mice. In this study, PBA and PAA concentrations were higher in the plasma than in other tissues. The concentrations of PBA and PAA were lowest in the lung compared to the concentrations in other tissues. The results from this study can help further research for the prevention and treatment of various ER stress-induced diseases.

## Acknowledgements

The author wishes to thank Dr. Yun-Jo Jung from Korea Basic Science Institute, Jeonju, Korea for his technical assistance. We thank Prof. Mie-Jae Lim from Research Center for Pulmonary Disorders, Chonbuk National University Medical School and Dr. Jin-Sung Kim for carefully editing our manuscript. This study was supported by research grant from the Korea Healthcare Technology, R&D project, Ministry for Health, Welfare and Family affairs (A 084144), South Korea.

## References


[1] M. Schroder, R.J. Kaufman, Mutat. Res. 569 (2005) 29–63.
[2] K. Zhang, Neurology 66 (2006) S102–S109.
[3] J.D. Lindholm, H. Wootz, L. Korhonen, Cell Death Differ. 13 (2006) 385–392.
[4] A. Azfer, J. Niu, L.M. Rogers, F.M. Adamski, P.E. Kolattukudy, Am. J. Physiol. Heart Circ. Physiol. 291 (2006) H1411–H1420.
[5] G. Liu, Y. Sun, Z. Li, T. Song, H. Wang, Y. Zhang, Biochem. Biophys. Res. Commun. 370 (2008) 651–656.
[6] K. Nagaraju, L.C. Rosen, I. Lundberg, R. Rawat, S. Cutting, R. Thapliya, J. Chang, S. Dwivedi, M. Mitsak, Y.W. Chen, P. Plotz, A. Rosen, E. Hoffman, N. Raben, Arthritis Rheum. 52 (2005) 1824–1835.
[7] U. Ozcan, E. Yilmaz, L. Ozcan, M. Furuhashi, E. Vaillancourt, R.O. Smith, C.Z. Gorgun, G.S. Hotarnisligil, Science 313 (2006) 1137–1140.
[8] C. Daosukho, Y. Chen, T. Noel, P. Sompol, R. Nithipongvanitch, J.M. Velez, T.D. Oberley, D.K. Clair, Free Radic. Biol. Med. 42 (2007) 1818–1825.
[9] S. Dasgupta, Y. Zhou, M. Jana, N.L. Banik, K. Pahan, J. Immunol. 170 (2003) 3874–3882.
[10] X. Qin, T. Hosoi, Y. OkumA., M. Kaneko, Y. Normura, Mol. Pharmacol. 66 (2004) 899–908.
[11] T. Mizukami, K. Orihashi, B. Herambang, S. Takahashi, M. Hamaishi, K. Okada, T. Sueda, J. Vasc. Surg. 52 (2010) 1580–1586.
[12] R.C. Rubenstein, P.L. Zeitlin, Am. J. Resp. Crit. Care Med. 157 (1998) 484–490.
[13] P.L. Zeithlin, M.D. West, R.C. Rubenstein, M.P. Boyle, C.K. Lee, E.L. Brass, Mol. Ther. 6 (2002) 119–126.
[14] B. Comte, T. Kasumov, B.A. Pierce, M.A. Puchowiczz, M.E. Scott, W. Dahms, D. Kerr, I. Nissim, H. Brunengraber, J. Mass Spectrom. 37 (2002) 581–590.
[15] S.W. Brusilow, J. Tinker, M.L. Batshaw, Science 207 (1980) 659.
[16] S.W. Brusilow, Pediatr. Res. 29 (1991) 119.
[17] T. Kasumov, L.L. Brunengraber, B. Comte, M.A. Puchowicz, K. Jobbins, K. Thomas, F. David, R. Kinman, S. Wehrili, W. Dahms, D. Kerr, I. Nissim, H. Brunengraber, Drug Metab. Dispos. 32 (2004) 10–19.
[18] S. Berg, B. Serabe, A. Aleksic, L. Bomgaars, L. McGuffey, R. Dauser, J. Durfee, J. Nuchtern, S. Blaney, Cancer Chemother. Pharmacol. 47 (2001) 385–390.
[19] S. Phuphanich, S.D. Baker, S.A. Grossman, K.A. Carson, M.R. Gilbert, J.D. Fisher, M.A. Carducci, Neurol. Oncol. 7 (2005) 177–182.
[20] M.A. Carducci, J. Gillbert, M.K. Bowling, D. Noe, M.A. Eisenberger, V. Sinibaldi, Y. Zabelina, T.L. Chen, L.B. Grochow, R.C. Donehower, Clin. Cancer Res. 7 (2001) 3047–3055.
[21] X. Yu, M.M. Thompson, D. Shi, M. Tulchman, Clin. Chem. 47 (2001) 351–354.
[22] C. Kennedy, K. Byth, C.L. Clarke, A. DeFazio, Mol. Cancer Ther. 1 (2002) 1025–1033.
[23] B.R.S. Hsu, S.T. Chen, S.H. Fu, Int. Immunopharmacol. 6 (2006) 1952–1959.